J Mol Neurosci (2007) 32:1–8
DOI 10.1007/s12031-007-0001-z

Tyr^{687} Dependent APP Endocytosis and Abeta Production

Sandra Rebelo · Sandra Isabel Vieira · Hermann Esselmann · Jens Wiltfang · Edgar F. da Cruz e Silva · Odete A. B. da Cruz e Silva

Received: 26 October 2006 / Accepted: 27 November 2006 / Published online: 5 April 2007

Abstract The neurotoxic Abeta peptide is derived by proteolytic processing from the Alzheimer's amyloid precursor protein (APP), whose short cytoplasmic domain contains several phosphorylatable amino acids. The latter can be phosphorylated 'in vitro' and 'in vivo,' and in some cases phosphorylation appears to be associated with the disease condition. Using APP-GFP fusion proteins to monitor APP processing, the role of Tyr^{687} was addressed by mimicking its constitutive phosphorylation (Y687E) and dephosphorylation (Y687F). Contrasting effects on subcellular APP distribution were observed. Y687E-APP-GFP was targeted to the membrane but could not be detected in transferrin containing vesicular structures, and exhibited a concomitant and dramatic decrease in Abeta production. In contrast, Y687F-APP-GFP was endocytosed similarly to wild type APP, but was relatively favoured for beta-secretase cleavage. Overall, Tyr^{687} appears to be a critical residue determining APP targeting and processing via different pathways, including endocytosis and retrograde transport. Significantly, from a disease perspective, mimicking Tyr^{687} phosphorylation resulted in a hitherto undescribed inhibition of Abeta production. Our results provide novel insights into the role of direct APP phosphorylation on APP targeting, processing and Abeta production.

Keywords APP phosphorylation · Tyr^{687} · Endocytosis · Abeta · APP processing

S. Rebelo · S. I. Vieira · O. A. B. da Cruz e Silva (✉)
Laboratório de Neurociências, Centro de Biologia Celular,
Universidade de Aveiro,
3810-193 Aveiro, Portugal
e-mail: odetecs@bio.ua.pt

H. Esselmann · J. Wiltfang
Molecular Neurobiology Laboratory, Department of Psychiatry and Psychotherapy, University of Erlangen-Nuremberg,
Erlangen, Germany

E. F. da Cruz e Silva
Laboratório de Transdução de Sinais, Centro de Biologia Celular,
Universidade de Aveiro,
Aveiro, Portugal

Introduction

Alzheimer's disease (AD) is progressive and multifactorial. One of the major pathological hallmarks is the presence of amyloid plaques, rich in Abeta peptides. The latter range from 37–42 amino acids, and result from the sequential proteolytic cleavage of the Alzheimer's Amyloid Precursor Protein (APP). APP can be cleaved by α-secretases [ADAM 10, ADAM 17 (TACE) and ADAM 9] at various subcellular locations, generating alpha cleaved sAPP ($_{\alpha}$sAPP), but can also be processed by β-secretases (BACE1 and BACE2) to yield beta cleaved sAPP ($_{\beta}$sAPP). Further cleavage by the γ-secretase complex (presenilin-1 or 2, nicastrin, aph1 and pen2) (Esler et al. 2002; Lee et al. 2000; Li et al. 2000a, b; Steiner et al. 2002; Verdile et al. 2006) produces either p3 or Abeta and the AICD (APP Intra-Cellular Domain) fragment comprising 50 amino acids (Bennett et al. 2000; Vassar et al. 1999; Yan et al. 2001). Abeta production can occur in the Golgi complex, especially in the trans-Golgi network (TGN), and to a lesser extent in the endoplasmic reticulum (ER). Abeta can also be produced in the endocytic pathway (Koo and Squazzo 1994; Nixon et al. 2001; Perez et al. 1999).

Although the precise function of APP is unclear, it exhibits characteristics of a signal transduction molecule. In fact,

several proteins (e.g. FE65) interact with the cytoplasmic domain of APP (Borg et al. 1999; Bressler et al. 1996; da Cruz e Silva et al. 2004a; Kinoshita et al. 2002; McLoughlin and Miller 1999; Sabo et al. 2001), forming large multimolecular complexes. The adaptor proteins direct APP to specific molecular pathways. Such interactions can be regulated by protein phosphorylation, as described for FE65 binding (Ando et al. 2001), and APP itself can be phosphorylated 'in vitro' and 'in vivo' (Ando et al. 2001; Oishi et al. 1997; Tarr et al. 2002; Zambrano et al. 2001). Lee et al. (2003) demonstrated that seven of the eight potentially phosphorylatable residues in the intracellular domain of APP were phosphorylated in AD patients, namely Tyr^{653}, Ser^{655}, Thr^{668}, Ser^{675}, Tyr^{682}, Thr^{686} and Tyr^{687}. The latter lies within the ^{682}YENPTY^{687} domain, a typical internalization signal for membrane-associated receptor proteins (Chen et al. 1990; Koo and Squazzo 1994; Lai et al. 1995), which conforms to a consensus sequence for coated-pit mediated internalization (Chen et al. 1990). This domain is of significant biophysical importance, bearing a characteristic type I β-turn (Kroenke et al. 1997; Ramelot et al. 2000), and central to protein–protein interactions, as for example with X11 (Ramelot et al. 2000) and Dab 1 (Homayouni et al. 1999). Thus, in the work here described we used a dynamic model system (da Cruz e Silva et al. 2004b) to evaluate the effect of mimicking Tyr^{687} phosphorylation. The data presented indicates that APP subcellular localization and incorporation into vesicular structures is Tyr^{687} dependent. In particular, the Y687E mutant, mimicking Tyr^{687} phosphorylation, failed to incorporate into visible endocytic vesicular structures and exhibited greatly reduced Abeta production in the conditioned media.

Materials and Methods

APP_{695} Expression Vectors

APP_{695} cDNA mutants were prepared to mimic a phosphorylated or dephosphorylated Tyr^{687} residue (glutamate or phenylalanine, respectively), using site directed mutagenesis (da Cruz e Silva and da Cruz e Silva 2003; da Cruz e Silva et al. 2004b). APP phosphorylation mimicking mutants and Wt-APP_{695} cDNAs were subcloned into appropriate vectors and their nucleotide sequences confirmed. Both mutant and Wt-APP_{695}-GFP fusions were engineered by PCR, removing the APP_{695} stop codon using specifically designed primers. The fusion constructs were produced by inserting the resultant fragments in frame into the pEGFP-N1 mammalian expression vector (Clontech, USA). The nucleotide sequences of the inserts were fully verified by DNA sequencing.

Cell Culture and Endocytosis Assays

Monkey kidney COS-7 cells were grown at 37°C and 5% CO_2 in Dulbecco's Modified Eagle's Medium (DMEM), supplemented with 10% foetal bovine serum, 100 U/ml penicillin, 100 mg/ml streptomycin and 3.7 g/l $NaHCO_3$, until 90% confluent (Rebelo et al. 2004). Transient transfections were performed using a cationic lipid transporter (LipofectAMINE 2000, Invitrogen Life Technologies). After 8 h, cells were divided into six-well plates with (for endocytosis analysis) or without (for Abeta quantification) coverslips pre-treated with 100 μg/ml polyornithine (Sigma, Portugal), and left to recover for 4 h. Cells were then incubated in serum-free DMEM supplemented with a protein synthesis inhibitor, 50 μg/ml cycloheximide (Sigma, Portugal), and processed as described below.

Transferrin endocytosis assays were performed on the transiently transfected cells essentially as previously described (Benmerah et al. 1998). Following a 2 h 15 min incubation period under the conditions described above, cells were washed with antimycotic/antibiotic-free DMEM. The endocytosis experiment was initiated by incubating cells for 30 min at 37°C with antimycotic/antibiotic-free DMEM supplemented with cycloheximide and with 20 mM HEPES, in order to eliminate endogenous transferrin. The medium was replaced with fresh medium supplemented with 1 mg/ml BSA and 100 nM Texas Red-conjugated transferrin (Molecular Probes, USA), and the cells were incubated for a further 15 min at 37°C (Benmerah et al. 1998). Cells were then immediately cooled to 4°C, washed twice in ice-cold PBS and fixed as described below.

Alternatively, an antibody uptake assay was also used to monitor APP internalization. COS-7 cells were transiently transfected, prepared as described above and incubated for 2 h. Cells were then washed twice with ice-cold PBS and incubated for 20 min on ice in serum-free DMEM supplemented with the 22C11 antibody (Chemicon, USA). Cells were subsequently washed three times with ice-cold PBS and then incubated at 37°C in DMEM supplemented with 10% foetal bovine serum for 0, 10, and 20 min. At each time point the cells were washed twice with PBS, fixed in 4% paraformaldehyde and processed for immunocytochemistry. Texas Red-conjugated anti-mouse IgG (Molecular Probes, USA) was used as a secondary antibody.

Abeta Analysis

Cells transfected with Wt or each of the mutant APP constructs were incubated for 3 h as described above. Abeta peptides were detected and quantitated essentially as previously described (Esselmann et al. 2004; Wiltfang et al. 2001). Conditioned media were immunoprecipitated using 25 μl dynabeads (Dynal, Germany) coated with 1E8 mAb

(Schering AG, Berlin). Immunoprecipitates were separated on 12% Bicine/Tris gels containing 8 M urea. Different Abeta peptide species were revealed by immunoblotting using mAb 1E8. Synthetic Abeta peptides were run in parallel for the identification of the different Abeta peptide species.

Immunoblots or the corresponding autoradiograms were scanned in a Molecular Imager (Bio-Rad, Portugal) and protein bands quantified using the manufacturer's Quantity One densitometry software. Data were expressed as mean ± SEM of determinations from at least three independent experiments. Statistical significance was conducted by one-way analysis of variance (ANOVA) with Tukey-Kramer test. Unless otherwise noted, a level of statistical significance is considered $P < 0.05$.

Results

Endocytosis Assays

Intracellular protein tracking was achieved by engineering APP_{695}-GFP fusion constructs, and the saturation of intracellular pathways due to protein overexpression was avoided by using relatively low transfection levels and by blocking 'de novo' protein synthesis (da Cruz e Silva et al. 2004b). In essence, COS-7 cells were transfected with wild type (Wt-APP_{695}-GFP) or either of the two Tyr^{687} mutant human APP cDNAs (Y687E-APP_{695}-GFP and Y687F-APP_{695}-GFP). Endocytosis and processing of mutant and wild type proteins was monitored as described above. Both Wt-APP-GFP and Y687F-APP-GFP were efficiently endocytosed, as demonstrated for both constructs by the speckled vesicular-like green fluorescent structures observed (Fig. 1a). The co-localization of APP_{695}-GFP green fluorescence and transferrin-Texas red fluorescence observed for Wt-APP-GFP and the dephospho-mimicking Y687F-APP-GFP mutant (Fig. 1c) revealed that transferrin was co-localizing with APP, thus reinforcing that both of these APP species are readily internalized. Interestingly, Y687F-APP-GFP appeared to be endocytosed approximately 1.5 × more efficiently than Wt-APP-GFP, as estimated by counting the number of co-localizing yellow vesicles detected (data not shown). In sharp contrast, the phospho-mimicking Y687E-APP-GFP mutant could not be detected in vesicular-like structures. This is evident in Fig. 1a, when fluorescence due to Y687E-APP-GFP alone is analysed or when the number of co-localizing yellow/orange vesicles are scored (Fig. 1c). In fact, the number of yellow/orange vesicles was dramatically reduced in cells transfected with Y687E-APP-GFP, leading us to conclude that this mutant protein is not efficiently endocytosed via clathrin-coated pits.

In order to assess if the green fluorescence detected in cytoplasmic vesicles was due to the presence of intact or truncated APP species, the internalization of the three proteins was further monitored by tracking their *N*- and *C*-termini during endocytosis using the antibody uptake assay described. At time 0 all cells revealed 22C11-staining at the cell surface (red fluorescence), although with a stronger intensity for Y687E-APP-GFP (Fig. 2A). Observation of the cells after 10 min at 37°C indicated that both Wt-APP-GFP and the Y687F-APP-GFP mutant were efficiently endocytosed (Fig. 2B), and the red (22C11) and green (APP-GFP) fluorescence co-localized extensively. Analysis of the GFP fluorescence alone also revealed that the two APP species are readily internalized. Noticeably, at this time point, many of the endocytic vesicles observed for Y687F-APP-GFP

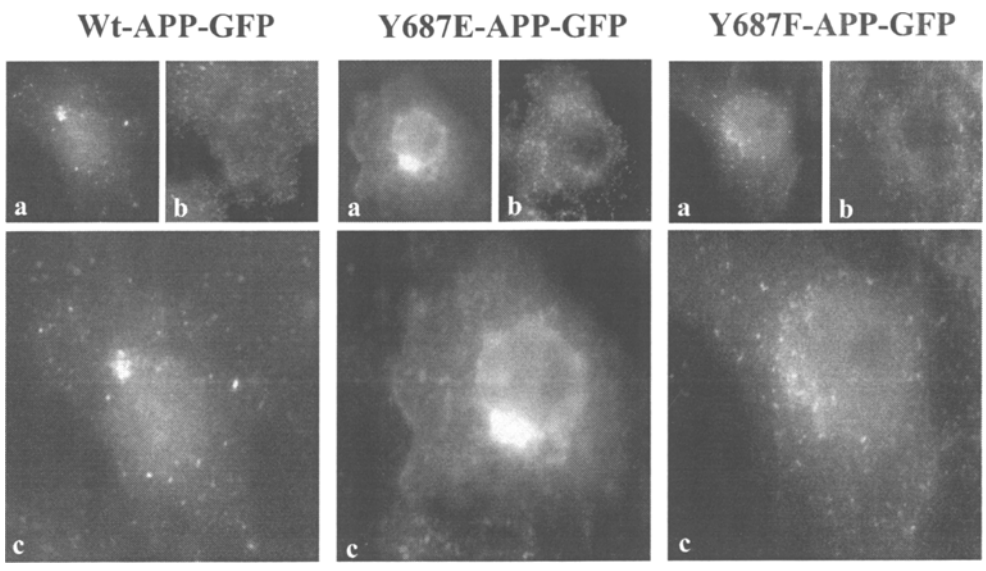

Fig. 1 Transferrin Assays. Internalization of Texas Red-conjugated transferrin was monitored in COS-7 cells transiently transfected with Wt-APP-GFP or either of the phospho-mimicking APP-GFP constructs. **a** APP-GFP fluorescence, **b** Transferrin-Texas red fluorescence, **c** Merged images of **a** and **b**

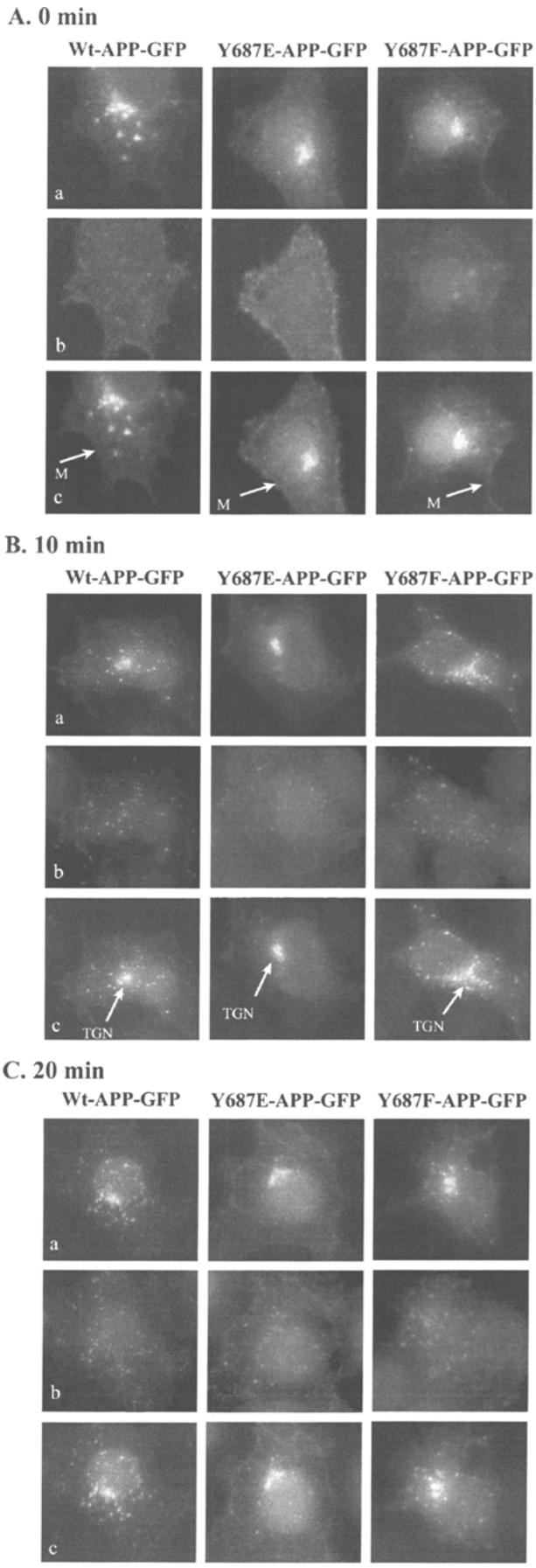

were already organized near the Golgi complex, consistent with Tyr^{687} dephosphorylated APP being endocytosed more efficiently/faster than Wt-APP-GFP. In contrast, the Y687E-APP-GFP mutant (mimicking phosphorylation) was not efficiently incorporated into vesicles and endocytosis of this mutant was not evident under our experimental conditions. Of note, the membrane staining remained intense, supporting poor endocytosis for this mutant (Fig. 2B). Unexpectedly, after 20 min at 37°C, Y687E-APP-GFP green fluorescence and the 22C11 staining were seen to co-localize in the vicinity of the TGN, suggesting that the phosphorylated protein may eventually also be internalized, albeit via a different route. On the other hand, and as for earlier time points, the Wt-APP-GFP and the Y687F-APP-GFP proteins continued to co-localize extensively in endocytic vesicles at 20 min. (Fig. 2C). Again, Y687F-APP-GFP appears to be more efficiently endocytosed and targeted for retrograde transport, as co-localization is clearly visible in the TGN. TGN co-localization for Wt-APP-GFP was much less marked. The Y687E-APP-GFP mutant, which as already mentioned is not visibly endocytosed, exhibits intense fluorescence at the cell membrane reinforcing that this mutant suffers impaired internalization (Fig. 2C). During the course of the experiment the vast majority of vesicles observed in cells expressing Y687E-APP-GFP stained red due to 22C11 binding to endogenously expressed APP, again supporting the hypothesis that this APP is not targeted to the vesicular structures normally visible.

Abeta Production

Abeta fragments secreted into the medium of cells transfected with the three constructs were quantitated as previously described (Esselmann et al. 2004; Wiltfang et al. 2001, 2002). This methodology allows for the separation, detection and quantitation of different Abeta species, including $Abeta_{1-37}$, $Abeta_{1-38}$, $Abeta_{1-39}$, $Abeta_{1-40}$, and $Abeta_{2-40}$. The results obtained with the three constructs are presented in Fig. 3. Y687F-APP-GFP and Wt-APP-GFP yielded a similar profile of Abeta production. Namely the Abeta species 1–37, 1–38, 1–39 and 1–40 were all clearly evident. A lower doublet (Fig. 3B) was also observed with the lower band co-migrating exactly with the $Abeta_{2-40}$ standard and the upper band was not defined. The Y687E-

◀**Fig. 2** Antibody Uptake Assays. The uptake of the 22C11 monoclonal antibody recognizing an epitope in the extracellular *N*-terminal domain of APP was monitored in COS-7 cells transiently transfected with Wt-APP-GFP or either of the phospho-mimicking APP-GFP constructs. Cells were monitored at 0 min (**A**), 10 min (**B**) and 20 min (**C**) after stimulation of antibody uptake. **a** APP-GFP fluorescence, **b** Transferrin-Texas red fluorescence, **c** Merged images of a and b. *M*—Plasma Membrane, *TGN*—Trans Golgi Network

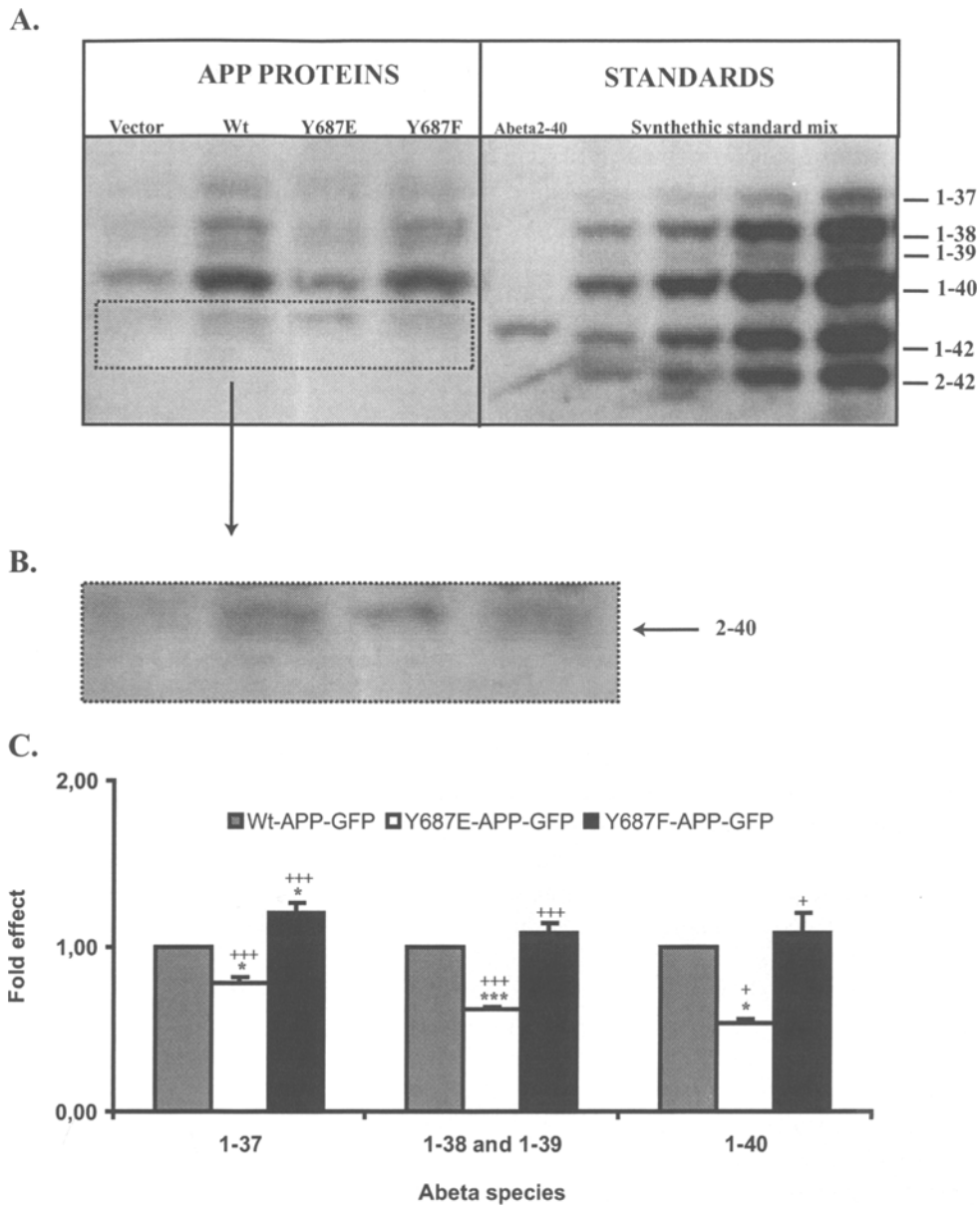

Fig. 3 Secretion of Abeta peptides. Conditioned media from cells transfected with one of the three constructs (Wt-APP-GFP, Y687E-APP-GFP and Y687F-APP-GFP) were collected and analyzed for Abeta production as described. Abeta production from endogenous APP was assessed from control cells transfected with the empty vector. Results were compared against a standard synthetic mix containing synthetic Abeta peptides of known size (**A**). The gel region corresponding to the $Abeta_{2-40}$ doublet was amplified (**B**). The intensities of the Abeta species observed (**C**) were quantified using a molecular imager with image analysis software (Quantity One)

APP-GFP protein, in contrast, produced significantly less of all Abeta species measured: $Abeta_{1-37}$ ($P < 0.05$), $Abeta_{1-38 \text{ and } 1-39}$ ($P < 0.001$) and $Abeta_{1-40}$ ($P < 0.05$), with $Abeta_{2-40}$ being almost completely absent (Fig. 3A–C).

Discussion

Protein phosphorylation as a regulatory mechanism in APP processing has been long been discussed (Gandy and Greengard 1994), however the precise molecular contributions have only recently began to be unravelled. In the work discussed here, low transfection levels and the use of cycloheximide to inhibit 'de novo' protein synthesis were vital to avoid overloading the normal APP processing pathways, thus allowing direct comparison of the intracellular localization of the Wt and Tyr^{687} phosphorylation site mutant APP-GFP proteins by epifluorescence. It is well established that APP has characteristics associated with cell surface receptors, can be re-internalized via clathrin-coated pits and be directed to the endosomal-lysosomal pathway. In our experimental system both Wt-APP-GFP and Y687F-APP-GFP were readily re-internalized via the endocytic pathway, with the 'dephosphorylated' mimicking protein being processed somewhat faster and more efficiently than the wild-type protein (Figs. 1, 2). In sharp contrast, the mutant mimicking phosphorylation on Tyr^{687}, Y687E-APP-GFP, was not incorporated into detectable vesicular structures (Figs. 1, 2), thus indicating that the membrane recycling of Y687E-APP-GFP is impaired. Nonetheless, the Y687E-APP-GFP protein was internalized, apparently via an alternative pathway which does not involve its incorpo-

ration into visible vesicles, as evidenced by the absence of the yellow/orange vesicular like structures, although yellow fluorescence could still be detected in the vicinity of the TGN (Fig. 2C). From our results, given the antagonic effects of mutating Try^{687} to Phenylalanine and Glutamate in comparison to the wild-type protein, it is reasonable to deduce that the phosphorylation state of Tyr^{687} results in the formation of different multimeric complexes which are differentially targeted. In fact, we have already initiated the analysis of the phosphorylation dependent APP interactome. An array of different APP binding proteins have been identified (unpublished data), depending on the residue of APP which is phosphorylated. This is not entirely unexpected if one considers for example that phosphorylation of APP at Thr^{668} affects its binding to FE65 (Nakaya and Suzuki 2006).

As a consequence of differential APP targeting, it appears that Tyr^{687} phosphorylated APP undergoes increased α-secretase processing, whereas its dephosphorylated counterpart appears to be relatively more favoured for β-secretase cleavage, as determined from sAPP production (data not shown). Direct measurement of Abeta secretion entirely supports this hypothesis (Fig. 3). Y687E-APP-GFP exhibited reduced Abeta production, with the almost complete absence of $Abeta_{2-40}$. Targeting and processing of APP via different pathways is important for Abeta production and the phosphorylation state of Tyr^{687} appears to be a critical determining factor. Hence, if one accepts that Y687E-APP-GFP mimics constitutive phosphorylation of Tyr^{687} and that Y687F-APP-GFP mimics its constitutive dephosphorylation, then it is reasonable to conclude that phosphoregulation of Tyr^{687} is an important regulatory mechanism not only for the incorporation of APP into endocytic vesicular structures and in regulating its transport from endosomes to the TGN, but this is also of consequence to APP proteolytic cleavages and Abeta production. Tyr^{687} phosphorylation has been described in samples from AD patients (Lee et al. 2003) where Abeta is found deposited in senile plaques. Hence, this appears contrary to what our results suggest, since Tyr^{687} phosphorylation produces less Abeta. However, one can envisage a protective endogenous mechanism at play, whereby Tyr^{687} phosphorylation reduces Abeta production, in a brain already producing excess of this toxic peptide. Notably, although Y687E-APP-GFP is not incorporated into visible vesicles, it is still processed, producing the other usual APP cleavage fragments. In fact, this partly explains why until now it has been difficult to detect differences in APP processing associated with direct phosphorylation of this intracellular domain. One is also forced to conclude that Y687E-APP is targeted and processed via an alternative pathway, potentially non-vesicular or otherwise involving vesicular structures/complexes below our detection limit. Of note, the simple measurement of APP proteolytic products provides no information as to the subcellular site of production and, indeed, they are likely to be produced at different subcellular locations. From our data it would appear that phospho-Tyr^{687} APP, although re-internalized to the ER and TGN, can still be cleaved by α-, β- and γ-secretases. This observation is consistent with the suggestion of Capell et al. (2005) that the γ-secretase complex could be completely assembled within the ER.

Our results showing that Abeta production can be modulated by direct APP phoshorylation may be of specific therapeutic relevance. It is interesting to note that the retrograde transport of BACE 1, responsible for the β-cleavage, is also regulated by the phosphorylation state of the protease (Wahle et al. 2005). Additionally, our conclusions favour the model that interaction of APP with its binding proteins may also be mediated by the phosphorylation state of APP itself (da Cruz e Silva et al. 2004a). Consequently, it may be possible to devise therapeutic strategies leading to decreased Abeta production, as observed here for Y687E-APP-GFP. Thus, signal transduction based diagnostics and therapeutics represent important future strategies of relevance to AD and other neurodegenerative diseases. The future identification of the kinases and phosphatases that act upon each of the APP phosphorylatable residues will likely prove useful in this respect.

Acknowledgements Supported by the EU V and VI Framework Programs (DIADEM and APOPIS), by the FCT (POCTI/CBO/34349/2001, POCTI/NSE/40682/2001 and POCTI/SAU-OBS/57394/2004) of the Portuguese Ministry of Science and Technology, and by CBC, Universidade de Aveiro. SR and SIV were recipients of PhD Fellowships (SFRH/BD/17693/2004 and Praxis XXI/BD/16218/1998).

JW was supported by grants from the German Federal Ministry of Education and Research (Competence Net Dementia, grant 01 GI 0420, Creutzfeldt-Jacob Disease Net, grant 01 GI 0301 and HBPP-NGFN2, grant 01 GR 0447).

References

Ando, K., Iijima, K. I., Elliot, J. I., Kirino, Y., & Suzuki, T. (2001). Phosphorylation-dependent regulation of the interaction of amyloid precursor protein with Fe65 affects the production of beta-amyloid. *Journal of Biological Chemistry, 276*, 40353–40361.

Benmerah, A., Lamaze, C., Begue, B., Schmid, S. L., Dautry-Varsat, A., & Cerf-Bensussan, N. (1998). AP-2/Eps15 interaction is required for receptor-mediated endocytosis. *Journal of Cell Biology, 140*, 1055–1062.

Bennett, B. D., Babu-Khan, S., Loeloff, R., Louis, J. C., Curran, E., Citron, M., et al. (2000). Expression analysis of BACE2 in brain and peripheral tissues. *Journal of Biological Chemistry, 275*, 20647–20651.

Borg, J. P., Lopez-Figueroa, M. O., de Taddeo-Borg, M., Kroon, D. E., Turner, R. S., Watson, S. J., et al. (1999). Molecular analysis of the X11-mLin-2/CASK complex in brain. *Journal of Neuroscience, 19*, 1307–1316.

Bressler, S. L., Gray, M. D., Sopher, B. L., Hu, Q., Hearn, M. G., Pham, D. G., et al. (1996). cDNA cloning and chromosome mapping of the human Fe65 gene: Interaction of the conserved cytoplasmic domains of the human beta-amyloid precursor protein and its homologues with the mouse Fe65 protein. *Human Molecular Genetics, 5*, 1589–1598.

Chen, W. J., Goldstein, J. L., & Brown, M. S. (1990). NPXY, a sequence often found in cytoplasmic tails, is required for coated pit-mediated internalization of the low-density lipoprotein receptor. *Journal of Biological Chemistry, 265*, 3116–3123.

Capell, A., Beher, D., Prokop, S., Steiner, H., Kaether, C., Shearman, M. S., et al. (2005). Gamma-secretase complex assembly within the early secretory pathway. *Journal of Biological Chemistry, 280*, 6471–6478.

da Cruz e Silva, E. F., & da Cruz e Silva, O. A. (2003). Protein phosphorylation and APP metabolism. *Neurochemical Research, 28*, 1553–1561.

da Cruz e Silva, O. A., Fardilha, M., Henriques, A. G., Rebelo, S., Vieira, S., & da Cruz e Silva, E. F. (2004a). Signal transduction therapeutics: Relevance for Alzheimer's disease. *Journal of Molecular Neuroscience, 23*, 123–142.

da Cruz e Silva, O. A., Vieira, S. I., Rebelo, S., & da Cruz e Silva, E. F. (2004b). A model system to study intracellular trafficking and processing of the Alzheimer's Amyloid Precursor Protein. *Neurodegenerative Diseases, 1*, 196–204.

Esler, W. P., Kimberly, W. T., Ostaszewski, B. L., Ye, W., Diehl, T. S., Selkoe, D. J., et al. (2002). Activity-dependent isolation of the presenilin-gamma-secretase complex reveals nicastrin and a gamma substrate. *Proceedings of the National Academy of Sciences of the United States of America, 99*, 2720–2725.

Esselmann, H., Maler, J. M., Kunz, N., Otto, M., Paul, S., Lewczuk, P., et al. (2004). Lithium decreases secretion of Aβ1-42 and C-truncated species Aβ1-37/38/39/40 in chicken telencephalic cultures but specifically increases intracellular Aβ1-38. *Neurodegenerative Diseases, 1*, 236–241.

Gandy, S., & Greengard, P. (1994). Regulated cleavage of the Alzheimer amyloid precursor protein: Molecular and cellular basis. *Biochimie, 76*, 300–303.

Homayouni, R., Rice, D. S., Sheldon, M., & Curran, T. (1999). Disabled-1 binds to the cytoplasmic domain of amyloid precursor-like protein 1. *Journal of Neuroscience, 19*, 7507–7515.

Kinoshita, A., Whelan, C. M., Berezovska, O., & Hyman, B. T. (2002). The gamma secretase-generated carboxyl-terminal domain of the amyloid precursor protein induces apoptosis via Tip60 in H4 cells. *Journal of Biological Chemistry, 277*, 28530–28536.

Koo, E. H., & Squazzo, S. L. (1994). Evidence that production and release of amyloid beta-protein involves the endocytic pathway. *Journal of Biological Chemistry, 269*, 17386–17389.

Kroenke, C. D., Ziemnicka-Kotula, D., Xu, J., Kotula, L., & Palmer, A. G. (1997). Solution conformations of a peptide containing the cytoplasmic domain sequence of the beta amyloid precursor protein. *Biochemistry, 36*, 8145–8152.

Lai, A., Sisodia, S. S., & Trowbridge, I. S. (1995). Characterization of sorting signals in the beta-amyloid precursor protein cytoplasmic domain. *Journal of Biological Chemistry, 270*, 3565–3573.

Lee, S. F., Shah, S., Li, H., Yu, C., Han, W., & Yu, G. (2000). Mammalian APH-1 interacts with presenilin and nicastrin and is required for intramembrane proteolysis of amyloid-beta precursor protein and Notch. *Journal of Biological Chemistry, 277*, 45013–45019.

Lee, M. S., Kao, S. C., Lemere, C. A., Xia, W., Tseng, H. C., Zhou, Y., et al. (2003). APP processing is regulated by cytoplasmic phosphorylation. *Journal of Cell Biology, 163*, 83–95.

Li, Y. M., Lai, M. T., Xu, M., Huang, Q., DiMuzio-Mower, J., Sardana, M. K., et al. (2000a). Presenilin 1 is linked with gamma-secretase activity in the detergent solubilized state. *Proceedings of the National Academy of Sciences of the United States of America, 97*, 6138–6143.

Li, Y. M., Xu, M., Lai, M. T., Huang, Q., Castro, J. L., DiMuzio-Mower, J., et al. (2000b). Photoactivated gamma-secretase inhibitors directed to the active site covalently label presenilin 1. *Nature, 405*, 689–694.

McLoughlin, D. M., & Miller, C. C. (1999). The intracellular cytoplasmic domain of the Alzheimer's disease amyloid precursor protein interacts with phosphotyrosine-binding domain proteins in the yeast two-hybrid system. *FEBS Letters, 397*, 197–200.

Nakaya, T., & Suzuki, T. (2006). Role of APP phosphorylation in FE65-dependent gene transactivation mediated by AICD. *Genes Cells, 11*, 633–645.

Nixon, R. A., Mathews, P. M., & Cataldo, A. M. (2001). The neuronal endosomal-lysosomal system in Alzheimer's disease. *Journal of Alzheimer's Disease, 3*, 97–107.

Oishi, M., Nairn, A. C., Czernik, A. J., Lim, G. S., Isohara, T., Gandy, et al. (1997). The cytoplasmic domain of Alzheimer's amyloid precursor protein is phosphorylated at Thr654, Ser655, and Thr668 in adult rat brain and cultured cells. *Molecular Medicine, 3*, 111–123.

Perez, R. G., Soriano, S., Hayes, J. D., Ostaszewski, B., Xia, W., Selkoe, D. J., et al. (1999). Mutagenesis identifies new signals for beta-amyloid precursor protein endocytosis, turnover, and the generation of secreted fragments, including Abeta42. *Journal of Biological Chemistry, 274*, 18851–18856.

Ramelot, T. A., Gentile, L. N., & Nicholson, L. K. (2000). Transient structure of the amyloid precursor protein cytoplasmic tail indicates preordering of structure for binding to cytosolic factors. *Biochemistry, 39*, 2714–2725.

Rebelo, S., Henriques, A. G., da Cruz E Silva, E. F., & da Cruz E Silva, A. O. B. (2004). Effect of cell density on intracellular levels of the Alzheimer's amyloid precursor protein. *Journal of Neuroscience Research, 76*, 406–414.

Sabo, S. L., Ikin, A. F., Buxbaum, J. D., & Greengard, P. (2001). The Alzheimer amyloid precursor protein (APP) and FE65, an APP-binding protein, regulate cell movement. *Journal of Cell Biology, 153*, 1403–1414.

Steiner, H., Winkler, E., Edbauer, D., Prokop, S., Basset, G., Yamasaki, A., et al. (2002). PEN-2 is an integral component of the gamma-secretase complex required for coordinated expression of presenilin and nicastrin. *Journal of Biological Chemistry, 277*, 39062–39065J.

Tarr, P. E., Contursi, C., Roncarati, R., Noviello, C., Ghersi, E., Scheinfeld, M. H., et al. (2002). Evidence for a role of the nerve growth factor receptor TrkA in tyrosine phosphorylation and processing of beta-APP. *Biochemical and Biophysical Research Communications, 295*, 324–329.

Vassar, R., Bennett, B. D., Babu-Khan, S., Kahn, S., Mendiaz, E. A., Denis, P., et al. (1999). Beta-secretase cleavage of Alzheimer's amyloid precursor protein by the transmembrane aspartic protease BACE. *Science, 286*, 735–741.

Verdile, G., Gandy, S. E., Martins, R. N. (2006). The Role of Presenilin and its Interacting Proteins in the Biogenesis of Alzheimer's Beta Amyloid. Neurochemical Research 2006 Aug 31, in press.

Wahle, T., Prager, K., Raffler, N., Haass, C., Famulok, M., & Walter, J. (2005). GGA proteins regulate retrograde transport of BACE1 from endosomes to the trans-Golgi network. *Molecular and Cellular Biochemistry, 29*, 453–461.

Wiltfang, J., Esselmann, H., Cupers, P., Neumann, M., Kretzschmar, H., Beyermann, M., et al. (2001). Elevation of beta-amyloid

peptide 2-42 in sporadic and familial Alzheimer's disease and its generation in PS1 knockout cells. *Journal of Biological Chemistry, 276*, 42645–42657.

Wiltfang, J., Esselmann, H., Bibl, M., Smirnov, A., Otto, M., Paul, S., et al. (2002). Highly conserved and disease-specific patterns of carboxyterminally truncated Abeta peptides 1-37/38/39 in addition to 1-40/42 in Alzheimer's disease and in patients with chronic neuroinflammation. *Journal of Neurochemistry, 81*, 481–496.

Yan, R., Munzner, J. B., Shuck, M. E., & Bienkowski, M. J. (2001). BACE2 functions as an alternative alpha-secretase in cells. *Journal of Biological Chemistry, 276*, 34019–34027.

Zambrano, N., Bruni, P., Minopoli, G., Mosca, R., Molino, D., Russo, C., et al. (2001). The beta-amyloid precursor protein APP is tyrosine-phosphorylated in cells expressing a constitutively active form of the Abl protoncogene. *Journal of Biological Chemistry, 276*, 19787–19792.